LDV measurement of bird ear vibrations to determine inner ear impedance and middle ear power flow

LDV Measurement of Bird Ear Vibrations to Determine Inner Ear Impedance and Middle Ear Power Flow

Pieter G.G. Muyshondt[1, a)], Felipe Pires[2, b)] and Joris J.J. Dirckx[1, c)]

[1]*University of Antwerp, Laboratory of Biophysics and Biomedical Physics, Groenenborgerlaan 171, 2020 Antwerp, Belgium*
[2]*Free University of Brussels, Department of Mechanical Engineering, Pleinlaan 2, 1050 Brussels, Belgium*

[a)]Corresponding author: pieter.muyshondt@uantwerpen.be
[b)]felipe.pires@uantwerpen.be
[c)]joris.dirckx@uantwerpen.be

Abstract. The mechanical behavior of the middle ear structures in birds and mammals is affected by the fluids in the inner ear (IE) that are present behind the oval window. In this study, the aim was to gather knowledge of the acoustic impedance of the IE in the ostrich, to be able to determine the effect on vibrations and power flow in the single-ossicle bird middle ear for future studies. To determine the IE impedance, vibrations of the ossicle were measured for both the quasi-static and acoustic stimulus frequencies. In the acoustic regime, vibrations were measured with a laser Doppler vibrometer and electromagnetic stimulation of the ossicle. The impedance of the inner ear could be determined by means of a simple RLC model in series, which resulted in a stiffness reactance of $K_{IE} = 0.20 \cdot 10^{12}$ Pa/m³, an inertial impedance of $M_{IE} = 0.652 \cdot 10^{6}$ Pa s²/m³, and a resistance of $R_{IE} = 1.57 \cdot 10^{9}$ Pa s/m. The measured impedance is found to be considerably smaller than what is found for the human IE.

1. INTRODUCTION

While the middle ear (ME) of mammals is made up of three hearing bones or ossicles, the avian ear has only one ossicle, which is called the columella. The function of the ME and the ossicles is to match the acoustic impedance of the outer ear in ambient air and the fluid-filled inner ear (IE) while transporting acoustic energy. To date, there are two conflicting theories regarding the motions of the avian columella: the first theory proposes that the ossicle performs side-to-side or rocking movements under stimulation of the eardrum [1], while the other theory proposes piston-like motions [2]. The nature of this motion is important because it influences the lever function of the ME that contributes to the impedance matching.

Studies in human [3] have shown that the IE influences motions of the stapes, which is the third hearing bone in mammals that is homologous to the avian columella. The predominant piston-like motions of the stapes footplate are partially converted into rocking motions at higher stimulus frequencies, probably due to the presence of the IE fluid behind the oval window. Also in pigeons, the impedance of the IE is assumed to affect columellar footplate vibrations [4]. To study the motions of the ossicles and the corresponding influence of the IE, measurements are needed of the IE impedance.

In humans, the acoustic impedance of the IE has been measured in several ways [5-6]. The IE impedance of birds is presumably very different from mammals because of differences in IE size and structure. The auditory portion of the IE, called the cochlea, is coiled in mammals, while in birds it is straight. Also, the architecture of the basilar membrane inside the cochlear duct is different, and the ratios of the surfaces of the round window and oval window are dissimilar, which are thought to contribute to the IE impedance as well.

In this study, the acoustic impedance of the avian IE is determined in the ostrich (*Struthio camelus*). In the acoustic frequency range, the IE impedance is determined by means of laser Doppler vibrometry and digital stroboscopic holography. As stimulation source, an electromagnetic induction solenoid and a magnet attached to the

ossicle are used. In the quasi-static regime, a piezo driver and a force transducer are used to measure the IE impedance, but these measurements are not a subject of the current paper.

2. METHODS

2.1 Acoustic impedance analysis

The method we used to measure the acoustic impedance of the IE (Z_{IE}) is similar to the approach followed in [5]. With this approach, the acoustic impedance of the columella and the IE combined (Z_{CIE}) is calculated from measurements of the columellar velocity v_C with intact IE, in response to stimulation forces measured at the distal end of the columella (F_C). The acoustic impedance is defined as

$$Z = \frac{p_C}{U_C} = \frac{F_C}{v_C A_{FP}^2}, \tag{1}$$

in which p_C is the pressure acting on the columella footplate, U_C the volume velocity of the footplate, and A_{FP} the total surface area of motion of the footplate. This area includes the medial surface area of the bony columellar footplate, but also a portion of the annular ligament that surrounds the footplate in the oval window and moves along with the footplate. The measurement procedure is repeated with an opened IE to determine the acoustic impedance of the columella Z_C, which incorporates the impedance of the bony ossicle and the annular ligament. The acoustic impedance of the IE (Z_{IE}) is then calculated by subtracting Z_C from Z_{CIE}.

With the followed approach, several assumptions are made: (1) motions of the columella are piston-like in the current setup, (2) forces (resp. velocities) measured on the columella are equal to the forces (resp. velocities) acting on the oval window, (3) velocities measured on the columella are in the linear response regime for the applied stimulus levels, and (4) the passive properties of the dead IE have not been altered after the sample preparations.

2.2 Sample preparation

Ostriches were chosen as model species as they are the largest existing avian species, which makes them very suited for manual handling during sample preparation. The heads of eight ostriches, with ages ranging from 1.5 to 5 years, were obtained from an ostrich farm. The samples were frozen one day after death and thawed right before measurement. Studies in human [6] have shown that it is possible for air to penetrate the IE during the freezing and thawing process, which may alter the IE impedance [5]. Therefore, each sample was checked for the presence of air bubbles behind the round window membrane before measurement. Subsequently, the ear canal, the eardrum and the cartilaginous extracolumella, which connects the eardrum to the columella, were removed. Also, half of the columellar shaft was cut from the distal side of the ossicle. To obtain optical access of the columella and the footplate, some of the surrounding tissue was removed, but without breaking up the IE structures. Finally, vibration measurements were performed after each of the following manipulations. First, the IE was left intact. Then, the round window membrane was perforated. Next, the IE was thoroughly drained with a suction tip through the perforation in the round window. Finally, the medial walls of the IE were drilled to remove the remaining IE fluid that was left on the medial surface of the columellar footplate.

2.3 Laser Doppler vibrometry

Since the oval window and the round window in the ostrich ear are positioned close together, it is unfeasible to acoustically isolate them from each other. If an acoustic source was chosen to stimulate the columella in the oval window as in [5], the round window would unavoidably be stimulated simultaneously by the generated pressure field. Therefore, an electromagnetic source was used to stimulate the columella exclusively.

A small gold-coated neodymium magnet with a mass of 3 mg was fixed with superglue on the tip of the remaining distal part of the columella. Then, a miniature copper induction solenoid was placed over the magnet with a translation stage to adjust the position of the coil in three directions. The force that the induction coil exerts on the electromagnet was calibrated using a balance with a precision of 0.1 mg. During the measurements, alternating sinusoidal currents were run through the coil to stimulate the magnet using stepwise frequencies increased between 0.3 and 4 kHz, with 16 lines per octave. At the same time, the induced vibration response of the columella was measured with a laser Doppler vibrometer (Polytec, OFV-534 & OFV-5000, Waldbronn, Germany) mounted on a

surgical microscope (OPMI Sensera/S7, Carl Zeiss, Jena, Germany). Vibrations of the columella were measured on the location of the electromagnet in a direction parallel to the columellar shaft and the induced magnetic field. To increase the reflection of the laser beam on the specimen, a small piece of reflective tape was placed on the top of the magnet. To control and analyze the stimulation and response signals, a program was developed in Matlab (Mathworks, Natick MA, USA) that interacts with a data acquisition device (National Instruments, USB-6251 BNC, Austin TX, USA) to generate the stimulus and measure the stimulation and response signals simultaneously. The data acquisition card was set at a sample rate of 48 kHz. Each signal was extended with 0.1 s to eliminate transient effects in the response. Subsequently, the amplitude of both signals and the phase difference between the two signals was determined from the Fourier transform of the waveforms at the applied stimulation frequencies. Electronic phase delays in the experimental setup were accounted for.

2.4 Digital stroboscopic holography

In order to determine the IE impedance with the laser vibrometry setup and the electromagnetic stimulation, the assumption had to be made that columellar displacements are piston-like. To verify this, the full-field displacements of the columellar footplate were measured with digital stroboscopic holography. Very short laser pulses (3 ns) were synchronized with the phase of a vibrating object, so that full-field displacements of the object's surface could be calculated at the chosen phase. By cycling these pulses stepwise through the vibration period, the entire time-dependent motion the surface was obtained. More details on the technique and the setup can be found in [7]. In the holography setup, the columella was stimulated electromagnetically in the same way as in the vibrometry setup, but the displacement response was measured from the medial side of the columellar footplate instead of from the lateral side. To expose the footplate, the IE needed to be removed for the measurements. To enhance reflectivity of the sample, the medial side of the footplate was coated with white make-up liquid (Kryolan Aquacolor Soft Cream - White Wet Make-up, Product Code 01129/00, Kryolan, Berlin, Germany).

2.5 Footplate surface area

According to Eq. (1), the acoustic impedance of the IE depends on the square of the total surface area of the footplate. We determined this area using microphotography, which will be discussed in detail in a forthcoming paper. An average surface area of (3.03 ± 0.41) mm² was found.

3. RESULTS

3.1 Laser Doppler vibrometry

Vibrometry measurements were made for stimulus frequencies between 0.3 and 4 kHz, with 16 lines per octave. The maximum frequency of 4 kHz was chosen in relation to the upper frequency limit of hearing in the emu (Dromaius novaehollandiae), which is a species closely related to the ostrich. The amplitude of the electromagnetic force stimulus was equal to 0.1 mN. Figure 1 shows the acoustic impedance calculated from the vibrometry measurements of (a) intact IE, (b) broken IE. Results from intermediate steps in the manipulation of the specimen are not shown.

When comparing the impedance of the intact and broken situation from Fig. 1 (a), it is seen that impedance magnitude values are consistently higher when the IE is still intact. Only at the lowest and highest frequencies shown, impedance magnitude values are similar. Peak amplitudes become sharper when the IE is broken, while being shifted to higher stimulus frequencies. This is also reflected in the phase response, in which the transition between -0.25 and +0.25 periods is much more sudden in the broken situation, although being postponed to higher frequencies. In the higher frequency range, the amplitude and phase both decrease for certain specimens with IE intact, but not with IE broken. Also, the variability in the measurements with IE intact is larger. For the impedance of the IE itself, we observe from Fig. 1 (b) that the amplitude and phase are similar to what is found in the intact situation in the middle frequency range. For lower and higher frequencies, the IE impedance deviates from the intact situation.

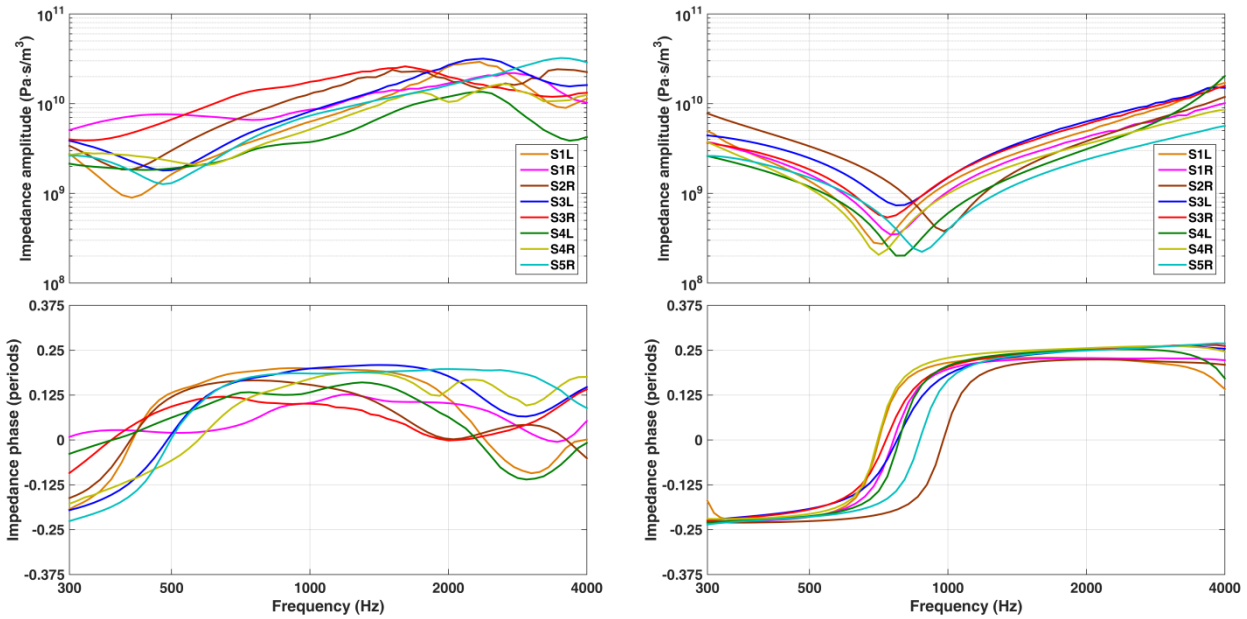

FIGURE 1. (a) Acoustic impedance amplitude (top) and phase (bottom) as a function of frequency, measured with (a) intact IE, (b) broken IE for the left and right ears of multiple specimens.

3.2 Digital stroboscopic holography

Holography measurements were made for frequencies from 0.05 kHz to 12.8 kHz, with 2 lines per octave. The chosen amplitudes of the stimulation force varied between 0.014 and 0.217 mN. Figure 2 shows the experimental results of the full-field footplate displacement in the right footplate of specimen 5, for two chosen stimulus frequencies of (a) 0.1 kHz and (b) 0.4 kHz with IE broken. Displacement amplitudes are normalized to the induced pressure of the electromagnetic stimulus, which was calculated from the force of the solenoid exerted on the magnet divided by the total area of motion at the footplate.

At 0.1 kHz, the footplate displacement contains two local maxima that have a relative phase difference of half a period, which shows that rocking motions are present in the vibrations of the columella in the current setup. This type of displacement pattern was seen for all measured frequencies between 0.05 and 0.3 kHz. Above 0.3 kHz, the displacement pattern altered, as shown in Fig. 2 (b) for 0.4 kHz. At this frequency, the full-field displacement magnitude and phase are largely uniform, which is also the case for higher stimulus frequencies. This indicates that displacements at frequencies above 0.3 kHz are mostly piston-like.

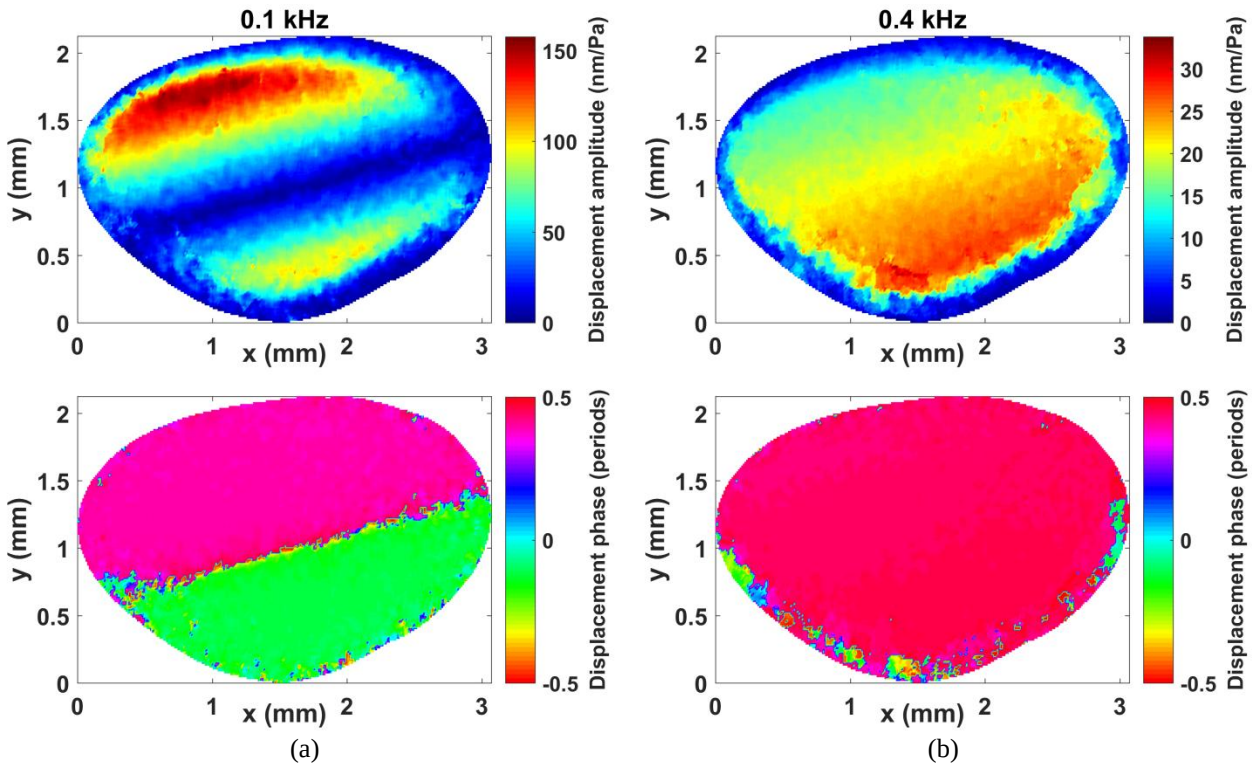

FIGURE 2. Full-field displacement response of the footplate in the right ear of specimen 5 with IE broken, at stimulus frequencies of (a) 0.1 kHz and (b) 0.4 kHz. Displacement amplitudes (top) are normalized to incident pressure and for the displacement phases (bottom) the reference phase was chosen arbitrary.

3.3 Acoustic impedance analysis

The mean of the acoustic impedance measurements is shown in Fig. 3 (a). As follows from the experiments, it is seen that measurement data is missing between 0.02 and 0.3 kHz. The mean of the experimental data was fitted for both IE intact and IE broken by using a simple RLC model in series, as was done in [5]. In this model, the impedance is described by three components, namely the stiffness reactance K that is dominant in the low frequency range, the inertial impedance M that is dominant in the high-frequency range, and the resistance R that dominates the impedance near the resonance frequency. Theoretically, K can be determined from the low-frequency response by $K = \omega\,\mathrm{Im}(Z)$, with ω a low-valued angular frequency and Z the impedance measured at that frequency. M can be found through $M = K/\omega^2$, with ω the resonance frequency in which the impedance phase becomes zero. R can be calculated from M at the resonance frequency via $R = \omega M/Q$, with Q the so-called Q-factor that is defined as the ratio of the resonance frequency to the half-power bandwidth. To obtain the best fit, the least-squares method was used to minimize the difference between the model and the experiment by varying the stiffness reactance K. The components M and R depend on K as defined in the current section. The weight given to each least-squares term is proportional to the number of measurements performed at the corresponding frequency.

The components of the impedance were found to be $K_{CIE} = 7.25{\cdot}10^{12}$ Pa/m³, $M_{CIE} = 0.952{\cdot}10^{6}$ Pa s²/m³ and $R_{CIE} = 2.02{\cdot}10^{9}$ Pa s/m³ for IE intact and $K_C = 7.05{\cdot}10^{12}$ Pa/m³, $M_C = 0.300{\cdot}10^{6}$ Pa s²/m³ and $R_C = 0.54{\cdot}10^{9}$ Pa s/m³ for IE broken. Then, the difference for each component was taken of the intact and broken data, resulting in the components of the IE impedance itself, being equal to $K_{IE} = 0.20{\cdot}10^{12}$ Pa/m³, $M_{IE} = 0.652{\cdot}10^{6}$ Pa s²/m³ and $R_{IE} = 1.57{\cdot}10^{9}$ Pa s/m³, for which the corresponding model is depicted in Fig. 3 (b).

In Fig. 3 (a) we observe that the amplitudes of both models slightly overestimate the low-frequency impedance, while underestimating the high-frequency impedance. We also observe that the impedances with IE intact and IE broken strongly overlap in the low-frequency range, which is the case for both the experiment and the model. Between 0.3 and 1 kHz, the resonance peaks are nicely reflected in the models. For frequencies above 2 kHz, the sudden drop in the IE impedance of the intact situation cannot be reproduced by the model. The same is found for

the impedance phase, in which the model fails to describe the intact IE for frequencies above 1 kHz. For IE broken, the phase is predicted well by the model. For the impedance of the IE, shown in Fig. 3 (b), the model describes the amplitudes well for low and middle frequencies, although it must be highlighted that standard deviations are large in the low-frequency range. For the highest frequencies above 1 kHz, the model is again unable to describe the experimental magnitude and phase.

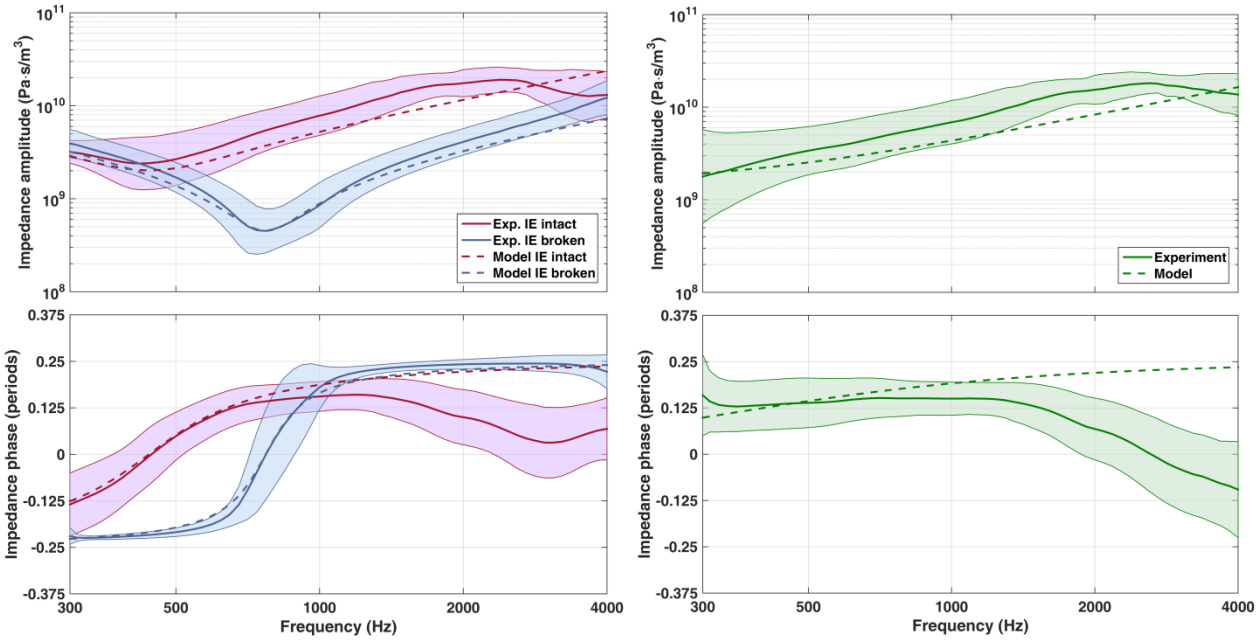

FIGURE 3. Acoustic impedance amplitude (top) and phase (bottom) for (a) the IE intact and broken, and (b) the IE itself as a function of frequency. The full lines represent the mean of the measurements at each frequency for IE intact (red), IE broken (blue) and IE impedance (green), with standard deviations plotted as colored bands. The corresponding RLC models are shown as dashed lines.

4. DISCUSSION

4.1 Method considerations

For measuring the vibration velocity of the columella to determine the IE impedance, the assumption was made that columellar footplate vibrations are piston-like. Below frequencies of 0.3 kHz, the full-field holographic data showed that the displacement contains two maxima that move out of phase, which indicates the presence of a vibration mode that goes along with rocking motions of the footplate. Apparently, small asymmetries in the geometry of the columella or the placement of the magnet or the coil may have caused the columella to vibrate asymmetrically at certain frequencies. Nevertheless, this technique has the advantage that we can make sure that only the oval window is stimulated and not the round window. With acoustic stimulation, the round window has to be acoustically isolated from the oval window.

4.2 Acoustic impedance

The acoustic impedance of the mammalian and human IE was estimated in previous studies, based on theoretical considerations [e.g. 8] and experimental data [e.g. 5-6]. Measurements of the ostrich ear in this study show that the avian IE impedance is much smaller than what is found in humans. The magnitudes found in this study are in the order of 10^9-10^{10} Pa s/m³, while in humans [5-6] the impedance values are one to two orders higher.

The components of the model impedance were calculated for IE intact (CIE), IE broken (C) and the difference of the two, representing the impedance of the IE itself (IE). The components are $K_{CIE} = 7.25 \cdot 10^{12}$ Pa/m³, $M_{CIE} = 0.952 \cdot 10^{6}$ Pa s²/m³ and $R_{CIE} = 2.02 \cdot 10^{9}$ Pa s/m³ for IE intact, $K_C = 7.05 \cdot 10^{12}$ Pa/m³, $M_C = 0.300 \cdot 10^{6}$ Pa s²/m³ and $R_C = 0.54 \cdot 10^{9}$ Pa s/m³ for IE broken, and $K_{IE} = 0.20 \cdot 10^{12}$ Pa/m³, $M_{IE} = 0.652 \cdot 10^{6}$ Pa s²/m³ and $R_{IE} = 1.57 \cdot 10^{9}$ Pa s/m³ for the IE itself. K_{IE} is nevertheless expected to be approximately zero, since the difference between IE intact and broken was negligible in the stiffness-dominated region of low frequencies. K_C represents the impedance of the columellar footplate and the annular ligament, while M_C represents the inertial impedance of the magnet and the footplate with annular ligament. The mechanical mass can be calculated from $m_C = M_C A_{FP}^2$, with A_{FP} the mean surface of motion of the footplate, resulting in 7.54 mg. The mass of the magnet was 3 mg, so the mass of the ligament and the remaining columella should equal 4.54 mg, which will be further investigated.

In [5], the impedance components of the human IE were found to be $K_{CIE} = 326 \cdot 10^{12}$ Pa/m³ and $R_{CIE} = 72 \cdot 10^{9}$ Pa s/m³ for IE intact (M_{CIE} was not considered in that study), and $K_C = 219 \cdot 10^{12}$ Pa/m³, $R_C = 5.7 \cdot 10^{9}$ Pa s/m³ and $M_C = 543 \cdot 10^{6}$ Pa s²/m³ for IE drained. When comparing each component, it can be concluded that acoustic impedances are consistently and considerably lower in the avian IE than in the mammalian IE. The differences in the size and structure of the IE in both classes of vertebrates seem to have their impact on IE impedance.

In future, the knowledge of the IE impedance that was acquired with this study will be appended to examine the influence of the IE structures on the vibration modes of the columella, and also on the power flow in the tympanic membrane and the middle ear.

5. CONCLUSION

Laser Doppler vibrometry allows us to measure the vibrations of the columella for determining the acoustic impedance of the IE of a bird in a frequency range of 0.3 up to 4 kHz. The acoustic impedance of the IE in the ostrich was fitted by means of an RLC model, resulting in a stiffness reactance of $K_{IE} = 0.20 \cdot 10^{12}$ Pa/m³, an inertial impedance of $M_{IE} = 0.652 \cdot 10^{6}$ Pa s²/m³ and a resistance of $R_{IE} = 1.57 \cdot 10^{9}$ Pa s/m³. These values are 1 to 2 orders in magnitude smaller than what is found in human [5]. Measurements of the acoustic IE impedance revealed that at low frequencies, the difference of the impedance with IE intact and IE broken is negligible. At high frequencies, the IE impedance cannot be described by a purely inertial component. The inertial impedance of the IE fluid is found to be smaller than total inertia of the fluid in the IE.

ACKNOWLEDGMENTS

The research was funded by the Research Foundation of Flanders (FWO), grant No. 11T9316N. We want to thank William Deblauwe and Fred Wiese for their technical assistance.

REFERENCES

1. E. P. Gaudin, *Acta Otolaryngol.* **65**, 316-326 (1968).
2. R. Norberg, *Phil. Trans. R. Soc.* **282 B**, 325-410 (1978).
3. N. Hato, S. Stenfelt, R. L. Goode, *Audiol. Neurotol.* **8 (3)**, 140-152 (2003).
4. A. W. Gummer, J. W. T. Smolders, R. Klinke, *Hear. Res.* **39**, 15-26 (1989).
5. S. N. Merchant, M. E. Ravicz, J. J. Rosowski, *Hear. Res.* **97 (1-2)**, 30-45 (1996).
6. R. Aibara, J. T. Welsh, S. Puria, R. L. Goode, *Hear. Res.* **152**, 100-109 (2001).
7. D. De Greef, J. A. M. Soons, J. J. J. Dirckx, *Int. J. Optomechatroni.* **8 (4)**, 275-291 (2014).
8. J. Zwislocki, *J. Acoust. Soc. Am.* **34**, 1514-1523 (1962).